Wiedemann-Franz Relation and Thermal-transistor Effect in Suspended Graphene

S. Yiğen and A. R. Champagne*
Department of Physics, Concordia University, Montréal, Québec, H4B 1R6, Canada
*E-mail: a.champagne@concordia.ca

Supporting Information

Supporting Information Contents

1. Sample Annealing

We annealed the samples using Joule heating *in situ* by flowing a large current in the devices (up to 540 and 837 μA for Samples A and B). Fig. S1 shows the 2-point dc transport data in Sample A before (red) and after (black) current annealing. Annealing and all subsequent measurements were done under high vacuum ≤10^{-6} Torr.

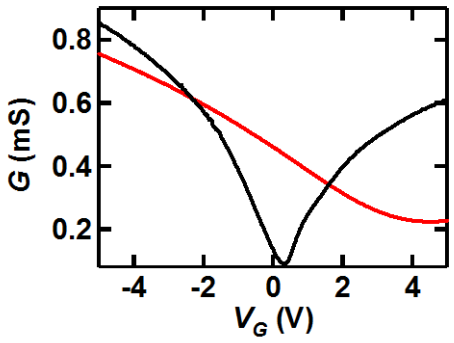

Figure S1: Sample annealing data. $G = I / V_B$ *vs* V_G data for Sample A before (red) and after (black) current annealing, $T \approx 20$ *K*.

2. Series Resistance: Upper Bound for Contact Resistance

An upper bound for the contact resistance, R_C, of our devices can be extracted from the two-point R-n_G curves. The data for Sample A is shown in Fig. S2. We fit the data with the expression [S1]

$$R = R_0 + \left[\frac{1}{\frac{n_G \mu W}{\ell} + G_{CNP}}\right] \quad \text{(S1)}$$

where R_0 is the resistance due to neutral scatterers plus R_C, ℓ is the length of the device, W the width, n_G the charge density induced by V_G, μ the mobility, and e the electron's charge. We fit the data at $T = T_e$ = 100 K, and for (V_G - V_D) > 1.3 V to avoid the thermal smearing around the Dirac point, V_D. The fit for the hole (electron) regime is shown as a light blue (red) dashed line in Fig. S2(a). The extracted mobility for Sample A in the doped regime is $\mu \approx 5.5 \times 10^4$ cm^2 / V.s at 100 K, and $R_0 \approx 477 \pm 53$ and 944 ± 80 Ω for hole and electron doping respectively. Panel (b) shows the conductance, $G = 1/R$, for Sample A before the series resistance R_0 is subtracted (black line) and after R_0 is subtracted for the hole (blue) and electron (red) doped data. The corrected conductance depends linearly on the gate induced charge density, n_G.

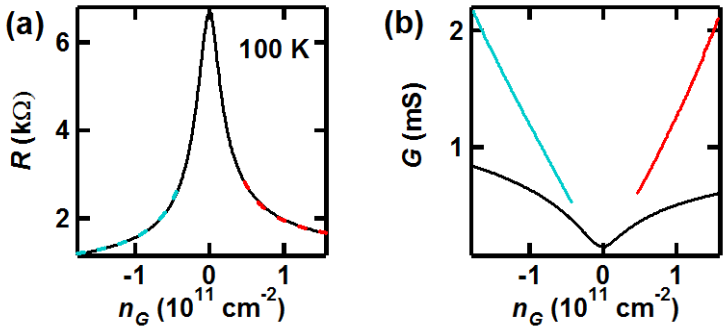

Figure S2: Extracting the series resistance in Sample A. (a) R-n_G data at 100 K for Sample A. The blue and red dashed lines are fits as described above from which the total series resistance, R_0, is extracted. (b) The same G-n_G data as in panel (a), before (black line) and after subtracting R_0 for holes (blue data) and electrons (red data).

3. Mean-free path of charge carriers

To extract an approximate elastic mean free path, l, for charge carriers, we consider doping due to impurities, n^*, and thermally activated carriers, $n_{th} = \left(\frac{\pi}{6}\right)\left(\frac{k_B T}{\hbar v_F}\right)^2$, where k_B is Boltzmann's constant, T the lattice temperature, $v_F = 10^6$ m/s the Fermi velocity. The total charge carrier density is [S2]

$$n_{tot} = n + p = \sqrt{n_G^2 + 4\left[\left(\frac{n^*}{2}\right)^2 + n_{th}^2\right]} \quad \text{(S1)}$$

where n_G is the charge density induced by the gate electrode. For instance, for Sample A at $T = 100$ K and V_G = -5.3 V (n_G = -1.8 x 10^{11} cm^{-2}) we find $n_{tot}(100\ \text{K}) \approx n_G$ and for Sample B at $T = 100$ K and V_G = 5.0 V (n_G = 1.1 x 10^{11} cm^{-2}) we find $n_{tot}(100\ \text{K}) \approx 1.15 \times 10^{11}$ cm^{-2}. We calculate a realistic estimate of the charge carrier mobility by using $\mu = \frac{\sigma}{n_{tot} e}$, where σ is the charge conductivity. At T = 100 K, μ = 3.6 and 2.9 x 10^4 cm^2/V.s using $R_c = R_0/2$ for Samples A (V_G = -5.3 V) and B (V_G = 5.0 V) respectively.

The extracted mobility decreases with T. From the mobility, we extract the mean-free path of the carriers as,

$$l = \sqrt{\frac{n_{tot}}{\pi}}\,\frac{h\mu}{2e} \qquad \text{(S2)}$$

At T = 100 K, we find l = 177 and 114 nm for A (V_G = -5.3 V) and B (V_G = 5.0 V), which is several times shorter than the length and width of the samples (650 nm x 675 nm for A, and 400 nm x 970 nm for B).

4. Joule self-heating data for Sample B

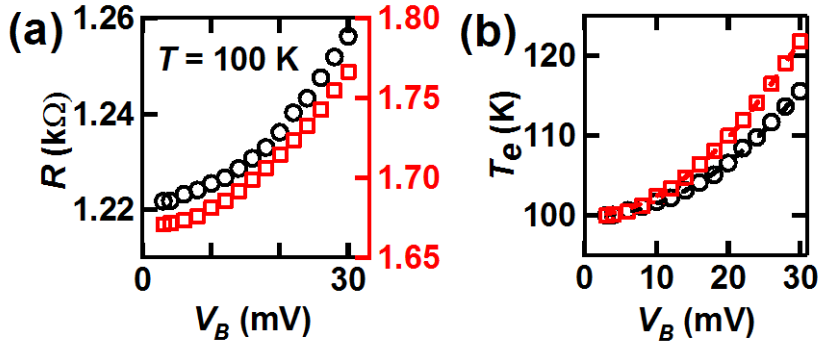

Figure S3: Electron heating in Sample B. (a) R vs V_B at T = 100 K for device B at V_G = 5 V (circle data, $n_{tot,\,T=0} \approx 1.1 \times 10^{11}$ cm^{-2}) and V_G = 2 V (square data, $n_{tot,\,T=0} \approx 0.5 \times 10^{11}$ cm^{-2}). Joule heating due to V_B raises the flake's average T_e above the cryostat T. (b) T_e vs V_B in Sample B at T = 100 K extracted from (a) using the thermometry curves as in Fig. 2(a). All of our K_e data is extracted with $V_B \lesssim 27$ mV. The solid lines in panel (b) are power law fit $T_e = 100 + BV_B^x$, and we find x =2.10 ± 0.03 and 1.99 ± 0.02, which is very close the expected x = 2 for Joule heating over a small T_e range.

5. Error analysis

To calculate the uncertainties on the values extracted for K_e, using Eq. S3 below, we account for four sources of uncertainty: error on the sample's length, $\Delta\ell$, width ΔW, resistance ΔR due to the contact resistance uncertainty ΔR_C, and extracted electronic temperature ΔT_e. We estimate $\Delta\ell$ = one mean free-path (extracted using Eq. S2) which ranges from 205 nm at 80 K (V_G = -5.3 V) to 158 nm at 150 K (V_G = -2.3 V) for Sample A and from 135 nm at 80 K (V_G = +5.0 V) to 87 nm at 150 K (V_G = -2.0 V) for sample B. $\Delta W \approx$ 50 nm, $\Delta R = \Delta R_C = R_0/2$ = 239 and 406 Ω for Samples A and B, and ΔT_e = the standard deviation of T_e from the fit of T_e vs V_B as shown in Figs. 2(d) and S3(b).

$$K_e = \frac{RI^2\ell}{12WH\Delta T} \qquad \text{(S3)}$$

The error on the measured current I is negligible compared to the other sources of error, and the thickness h = 0.335 nm is a standard value used by all experiments and theory. Note that $\Delta T = T_e - T$ where T is the cryostat temperature. The error on T is about 0.1 K

and comes from the accuracy of our temperature controller, thus the error on ΔT is roughly ΔT_e + 0.1 K. We calculate ΔK_e using Eq. S4,

$$\frac{\Delta K_e}{K_e} = \sqrt{\left(\frac{\Delta \ell}{\ell}\right)^2 + \left(\frac{\Delta W}{W}\right)^2 + \left(\frac{\Delta R}{R}\right)^2 + \left(\frac{\Delta(\Delta T)}{\Delta T}\right)^2} \quad \text{(S4)}$$

The calculated errors are shown in Figs. 3 and 4. For example, the error bars $\Delta K_e/K_e$ at T = 100 K are approximately 20% for Samples A and 40% for Sample B.

6. Contact resistance effect on extracted Lorenz numbers

The uncertainty on the contact resistance does not significantly affect the accuracy of the agreement of the data in Fig. 3 of the main text with the Wiedemann-Franz relation. We used $R_C = R_0/2$ = 239 and 406 Ω for Samples A and B respectively in Fig. 3. Figures S4 (below) and 3 (main text) show that the quality of the fit of the data to the WF law is not affected by the systematic uncertainty on R_C. The only effect of the R_C uncertainty is a quantitative change in the extracted Lorenz number L. Fig. S4(a) shows the WF law fit to the data if we let $R_C = R_{min}$ = 120 Ω (calculated using the lowest reported gold-graphene resistance [S3] at similar densities), and Fig. S4(b) shows the WF law fit to the data if we let $R_C = R_{max}$ = 477 Ω (extracted in SI section 2).

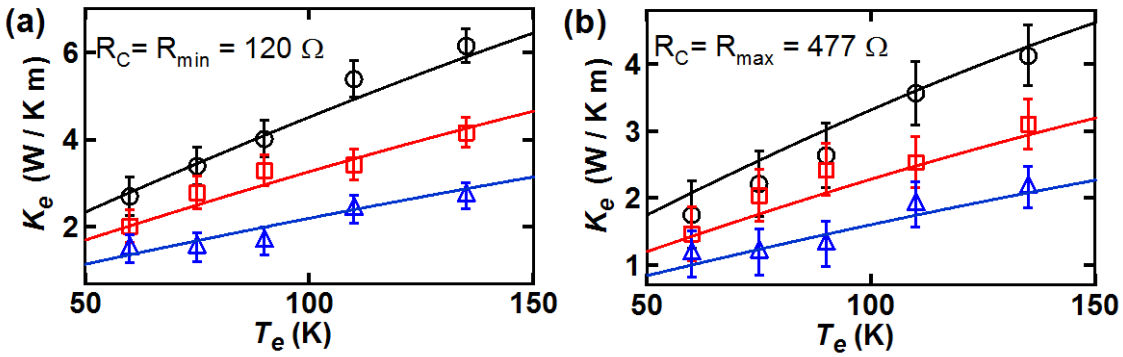

Figure S4: Effect of the contact resistance uncertainty on data in Fig. 3(a). The electronic thermal conductivity, K_e, of Sample A in the hole-doped regime vs T_e for $\Delta T = T_e - T$ = 10 K. The circle, square and triangle data show K_e at V_G = -5.3, -3.3 and -2.3 V respectively corresponding to $n_{tot,\ T=0} \approx$ -1.8, -1.1, -0.8 x 10^{11} cm^{-2}. (a) Using $R_C = R_{min}$ = 120 Ω. The solid lines are given by the WF relation $K_{WF} = L\sigma T_e$ with L = 0.53, 0.64 and 0.68 x L_o respectively. (b) Using $R_C = R_{max}$ = 477 Ω. The solid lines are given by the WF relation with L = 0.33 x L_o for all three curves.

REFERENCES

[1] C.R. Dean, *el al.*, *Nature Nanotechnol*. **5**, 722 (2010).
[2] V. E. Dorgan, M. H. Bae, and E. Pop, *Appl. Phys. Lett.* **97**, 082112 (2010).
[3] R. Ifuku, K. Nagashio, T. Nishimura, and A. Toriumi, *arXiv:1307.0690* (2013).